INTERNATIONAL JOURNAL OF
MARITIME TECHNOLOGY
IJMT Vol.9/ Winter 2018 (33-40)

Available online at http://ijmt.ir/browse.php?a_code=A-10-194-1&sid=1&slc_lang=en

Resistance Prediction for a Novel Trimaran with Wave Piercing Bow

Karim Akbari Vakilabadi[1*], Mohammad Reza Khedmati[2], Abbas HasanAbadi[3], Alireza Mohammadi[3]

[1]Marine Faculty of Imam Khomeini Maritime University, Nowshahr-,Iran, Assistant Professor, Akbari.karim@gmail.com(Corresponding Author)
[2]Department of Maritime Engineering of Amirkabir University of Technology, Tehran, Iran, Professor, Khedmati@aut.ac.ir
[3]Marine Faculty of Imam Khomeini Maritime University, Nowshahr-, Iran, Lecturer, Msc,alireza.or.mohammadi@gmail.com, hasanabad74@gmail.com

ARTICLE INFO

Article History:
Received: 13 May.2017
Accepted: 6 Feb. 2018

Keywords:
Trimaran
Resistance
Piercing Bow
Experiment

ABSTRACT

Dynamic behaviour of a trimaran vessel is investigated in this study. The body of the trimaran is composed of a centre hull with a quite slender wave piercing bow profile (a length-to-width ratio of 12.96) and two outriggers with Wigley mathematical body. Trimaran hull form and motion have been extensively studied due to the development of numerical and analytical methods as well as the exploitation of experimental setup. In this article, we investigate the possibility to move the side hulls longitudinal and transversal with respect to the main hull in order to find the optimum situation for minimum drag. The mathematical approach is numerical method CFD with the help of VOF. Moreover the experimental measurement was provided for some cases. The simulation results indicated good agreement with the experimental results. The investigations undertaken within the scope of this article provide a starting point to investigate the flow pattern and performance of such ships.

1. Introduction

There is an increased interest in trimaran vessels due to its advantages and applications (Elcin 2003). Because of the stability gained from the side hulls, the trimaran can use slender hulls that reduce residuary resistance. As a consequence, the trimaran reduces fuel consumption compared to an equivalent monohull. The trimaran's three hulls have the flexibility to accommodate many propulsion plant arrangements. An important feature of the trimaran form is the additional upper deck and upper ship space that is created. For the same displacement or volume as a monohull, the trimaran form will generate a ship with a greater length and, in the useful central region, greater upper deck beam that is extreme breadth between the two side hulls, giving the possibility for many potential uses. The trimaran may offer desirable motions performance. The long, slender waterline of the main hull provides excellent seakeeping performance, benefit from the added collision protection and damaged stability, the use of the side hulls as armor for critical machinery and control spaces in the case of war vessels. The trimaran hull form offers major advantages in signature reduction to warship designers.

Hebblewhiteetals. (2007) investigated the effects of the longitudinal stagger of the side hulls (outriggers) with respect to the center hull on the motions in heave and pitch of a representative trimaran hull.

K. A. Vakilabadi et al.(2014) Investigated the Dynamic behaviour of a trimaran vessel. The literature survey indicates that, to date, investigations on trimaran hull forms have been confined to determining the effects of transverse and longitudinal positions of the side hulls mainly on the resistance and powering characteristics. Javanmardietals. (2008) investigated the hydrodynamic resistance and maneuvering of a trimaran with Wigley body form using a CFD code. The results showed that for trimaran configuration when the three bow hulls are aligned, as the speed increases, the rate of total drag growth will decrease, because the length of interaction between the waves created by the main hull with outriggers decreases. Resistance decreases with increasing transverse distance where three hulls bow are aligned, but increasing transverse distance does not affect where three bodies stern are aligned. The work also underlined that hydrodynamic resistance is an important factor for trimaran design, but factors such as maneuverability and seakeeping are also considerable.

[Downloaded from ijmt.ir on 2026-11-25]

Outriggers position has great effect on trimaran maneuverability. When the bow of three bodies are aligned, the maneuvering quality is not good, because in this case, vessel trim causes outriggers to come out from water. Therefore motion stability decreases. Other configurations have almost the same turning circles diameter. But from resistance point of view, when the stern of three hulls are aligned, less thrust force is necessary, so it is more effective than other configurations. I. Mizineetals. (2009) studied a large Trimaran ship - Heavy Air Lift Support Ship (HALSS) showing a large change in resistance (70%) due to a moderate (15% from length of center hull) shift in the longitudinal side hull position. The work also focused on the influence of the skegs on the stern flow, understood with the aid of several Computational Fluid Dynamics calculations performed with various computational codes and compared to model test data. Ni etals. (2011) noticed that since trim and sinkage are significant while vessels are advancing forward with high speed, the predicted vessel resistance based on restrained model theory or experiment may not be real resistance of vessels during voyage. They found it necessary to take the influence of hull gesture into account for predicting the resistance of high-speed ship. They treated the resistance problem of high speed ship with the viscous flow theory, and adapted the dynamic mesh technique to coincide with variation of hull gesture of high speed vessel on voyage. The simulation of the models of S60 ship and a trimaran moving in towing tank with high speed corresponded to the experimental data, indicating that the resistance prediction for high speed vessels should take hull gesture into consideration and the dynamic mesh method proposed was effective in calculating the resistance of high speed vessels. H. Zeraatgar et al.(2011) studied a squat for vessels with Series-60 hull forms in shallow water. When a ship moves in the shallow waters, the velocity of the fluid flow at the bottom of the ship increases and the pressure decreases which in turn leads to the decrease of buoyancy force and the increase of the resistance by increasing in ship draught. The scope of the present work is to move the lateral hull in X (longitudinal) and Y (transversal) direction (Y1 and Y2) to find the best position regarding the least drag. The trimaran velocity varies with the non-dimensional Froude number(Frn): 0.15, 0.3 , 0.45, 0.6, 0.75 , 0.9 and 1. The simulation was performed with the VOF method

2. Description of the Model

"Wave piercing bow" profile (Figure 1) has two advantages: improving the hydrodynamic performance as well as simplifying the construction process [1-2]: The simplifying construction process includes %15 decrease in labour engagement, %50 decrease in assembly, welding and bending expenses (due to its simplicity%15 decrease in alignment process operation and eventually there is a potential of being automatically welded [1-2]; The significant improvement of "wave piercing bow" profile includes higher energy-efficient characteristic in waves, higher transit speed, reduced power consumption, improved fuel efficiency, increased operational time, increased schedule-keeping, elimination of slamming and bow impact, soft entry in waves, less spray, low acceleration levels, reduced vibration levels, increased comfort and available crew rest time, safer workplace due to smoother motions and protection provided by hull [1-3]. To fabricate the model the fibre reinforced plastic was exploited. The model was made with a scale factor of according to ITTC 7.5-01-01-01. The hull form was modelled up to the main deck level and no appendages were fitted. Length between perpendicular and service speed of the vessel are equal to 124 m and 25 knots, respectively. These features correspond to the Froude number of 0.368. Figure 2 shows transverse sectional view of the main hull as well as the supporting side hulls; Table 1 presents the principal dimensions of the prototype vessel and its scaled modelwith scale factor λ=80, while the body lines are shown in Figure 3.

The model has been built up to the main deck omitting shaft, propeller, steering and propulsion systems. In order to separate inertia forces from hydrodynamic forces, before each test, draft and trim values must be adjusted to compensate the distribution of weight and inertia forces in the model. Thus, location of centre of gravity and the values of gyration radii must be known. The model is loaded and ballasted in such a way that the values of Vertical position of Centre of Gravity (VCG), Longitudinal position of Centre of Gravity (LCG) and also radii of gyration for both pitch and roll motions can be easily reached. Location of centre of gravity for the model was determined using suspension method, Figure 4(a). Moreover, Biffilar method [21] was used to determine the radii of gyration in air, Figure 4(b). Radius of gyration is found to be equal to 0.387 m for pitch motion (about 25 percent of water line length) and 0.095 m for roll motion (about 35 percent of overall beam).



Figure. 1 The centre (main) hull's wave piercing bow profile

[Downloaded from ijmt.ir on 2026-11-25]

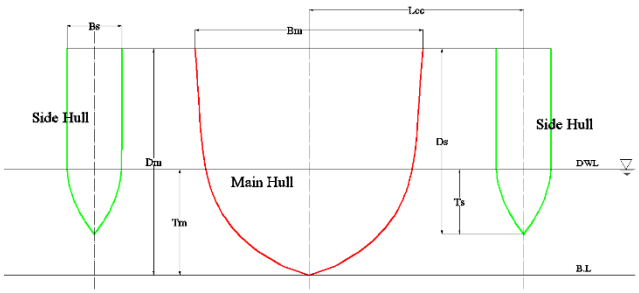


Figure. 2 Transverse sectional view of the main hull and its supporting side hulls

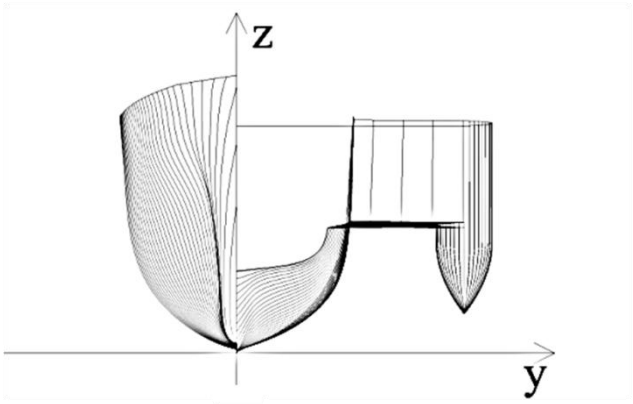


Figure. 3 Body lines and general layout of the trimaran vessel and its scaled model



centre hull side hull trimaran model

(a)



(b)

Figure. 2 (a) Application of the suspension method to determine the model's centre of gravity , (b) Application of Biffilar method for determination of radii of gyration



Figure. 3 Towing tank facilities of the Marine Research Centre (MRC) at the Sharif University of Technology (SUT)

Table 1. The principal dimensions of prototype trimaran and its scaled modelwith scale factor λ=80

Characteristic[unit]	Model
Length overall [m]	1.55
Length on waterline [m]	1.54
Beam overall [m]	27.22×10^{-2}
Beam on waterline [m]	12×10^{-2}
Depth [m]	14.72×10^{-2}
Draught [m]	5.48×10^{-2}
Length of side hull [m]	45×10^{-2}
Beam of side hull [m]	2.95×10^{-2}
Depth of side hull [m]	10.17×10^{-2}
Draft of side hull [m]	0.93×10^{-2}
Clearance between centreline of main and side hull [m]	12.125×10^{-2}
Displacement [ton]	4.39×10^{-3}

3. Experimental Set-Up

The experimental program was performed exploiting the towing tank facilities of Marine Research Centre (MRC) at Sharif University of Technology (SUT), Figure 5. The towing tank includes three basic parts: the tank, the computerized towing system and the wave generator. Length and width of the tank are 24 m and 2.5 m, respectively (see Table 2). Wave generator is able to produce either regular or irregular waves with length of 0.3 m to 2.8 m and maximum amplitude of 0.1 m. In order to damp the waves a wave damper is contrived at the end of the tank. The Labview software was developed to acquire the measured hull's motions.

Table 1. Main particulars of the towing tank of MRC at (SUT)

Characteristic	Value
Length	25 [m]
Width	2.5 [m]
Depth	1.2 [m]
Maximum speed of carriage	6 [m/s]
Maximum acceleration of carriage	2 [m/s2]
Towing system	Electromotor [4kw]

4. Experimental Program

A series of resistance tests in calm water is conducted on the trimaran model in order to identify the total

[Downloaded from ijmt.ir on 2026-11-25]

resistance. The displacement of the model is determined considering the displacement of the prototype vessel (2248 ton). Other conditions such as trim and draft are also established so that the real design conditions of the vessel are fulfilled. Maximum speed of the model is equal to 2 m/s corresponding to the speed of 35 knots of the prototype vessel. Figure 6 shows a typical testing situation.

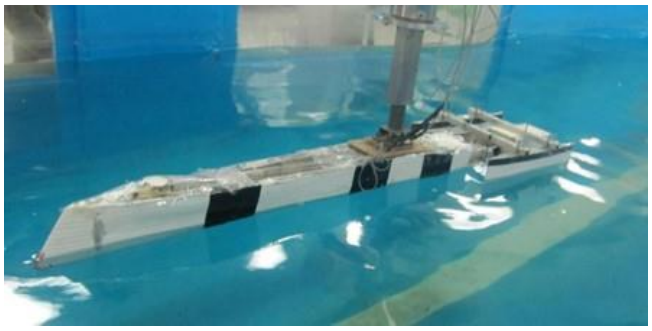


Figure. 6 Model during resistance test under head sea condition (model speed=0.5 m/s)

Every test is repeated 3 times to assure the validity of the test results. In addition to visual control of water surface, tests are carried out with 15 minutes delay for the water surface to calm down.

5. Numerical Model

The Reynolds average Navier stokes equation were used within this study to numerically model the flow characteristic around the trimaran:

$$\frac{\partial \rho}{\partial t}+\frac{\partial(\rho u_i)}{x_i}=0\ (i=1,2,3) \tag{1}$$

$$\frac{\partial(\rho u_i)}{\partial t}+\frac{\partial(\rho u_i u_j)}{\partial x_j}=\frac{\partial}{\partial x_j}\left[\mu\left(\frac{\partial u_i}{\partial x_j}+\frac{\partial u_j}{\partial x_i}-\frac{2}{3}\delta_{ij}\frac{\partial u_i}{\partial x_j}\right)\right]-\frac{\partial p}{\partial x_j}+\frac{\partial(-\rho\overline{u_i u_j})}{\partial x_j} \tag{2}$$

$$\rho=\sum_{n=1}^{2}\alpha_n\rho_n \tag{3}$$

$$\mu=\sum_{n=1}^{2}\alpha_n\mu_n \tag{4}$$

Where t is time, ρ is the density, μ is the dynamic viscosity, n is the fluid phase number, α is the phase fraction and $-\rho\overline{u_i u_j}$ is the turbulent Reynolds stress (τ_{ij}).

$$-\rho\overline{u_i u_j}=\mu_t\left(\frac{\partial u_i}{\partial x_j}+\frac{\partial u_j}{\partial x_i}\right)-\frac{2}{3}\left(\rho k+\mu_t\frac{\partial u_i}{\partial x_j}\right) \tag{5}$$

Where μ_t is turbulent viscosity, k is the turbulent kinetic energy.

To solve such problem the standard $k-\varepsilon$ model is used within this study through the following equations:

$$\frac{\partial(\rho k)}{\partial t}+\frac{\partial(\rho u_i k)}{\partial x_i}=\frac{\partial}{\partial x_j}\left[\left(\mu+\frac{\mu_t}{\sigma_k}\right)\frac{\partial k}{\partial x_j}\right]+P_k-\rho\varepsilon+S_k \tag{6}$$

$$\frac{\partial(\rho\varepsilon)}{\rho t}+\frac{\partial(\rho u_i\varepsilon)}{\partial x_i}=\frac{\partial}{\partial x_j}\left[\left(\mu+\frac{\mu_t}{\sigma_\varepsilon}\right)\right]\frac{\partial\varepsilon}{\partial x_j}+C_{1\varepsilon}\frac{\varepsilon}{k}P_k-C_{2\varepsilon}\rho\frac{\varepsilon^2}{k}+S_\varepsilon \tag{7}$$

Where the dissipation of turbulent kinetic energy is ε, P_k is the production of turbulent kinetic energy, S_k and S_ε are source terms and μ_t is the dynamic turbulent viscosity. P_k And μ_t are as follow:

$$\mu_t=\rho C_\mu\frac{k^2}{\varepsilon} \tag{8}$$

$$P_k=-\rho\overline{u_i u_j}\frac{\partial u_j}{\partial x_i} \tag{9}$$

Where:

$$C_{1\varepsilon}=1.44,\ C_{2\varepsilon}=1.92,\ C_\mu=0.99,\ \sigma_k=1,\ \sigma_\varepsilon=1.3 \tag{10}$$

These set of equations are solved via Fluent code. The interpolation methods used are as follow:

SIMPLE method for Pressure-Velocity Coupling, Green-Gauss cell based for Gradient, PRESTO! For pressure, second order upwind for Momentum, QUICK for Volume Fraction, Second order Upwind for Turbulent Kinetic energy and turbulent dissipation rate. For the simulation of the free surface and also capturing the wave pattern a volume of fluid method (VOF) is used. Through this method every cell is considered to be occupied with two fluids: water and air with a volume fraction α which satisfies the following equation:

$$\sum_{n=1}^{2}\alpha_n=1 \tag{11}$$

Every transport variable (ψ) is represented by the phase fraction through the following equation:

$$\psi=\sum_{n=1}^{2}\alpha_n\psi_n \tag{12}$$

5.1 Boundary Condition and Mesh Density Analysis

The trimaran was modelled in a numerical domain consisting of water and air. The air and water have a common surface at the level of 4.5 m above the lowest part of the trimaran. The inlet is divided into two inlet conditions: air inlet velocity and water inlet velocity, the outlet is thoroughly defined as outflow. The two phases of fluid, air and water is treated with multiphase mixture model in Fluent. The volume of fluid (VOF) approach is responsible to capture the two phase fluid behaviour specifically at the interface level. Grid sensitivities were performed to ensure the reliability of the numerical model. Namely, the most important parameter of this study i.e. the drag force was adopted as controlled variable. The mesh density was progressively increased but the quantities changed less

[Downloaded from ijmt.ir on 2026-11-25]

than 3%. According to the sensitivity analysis, a final mesh of approximately 450K elements was adopted for the simulations.

6. Results and Discussion

The experimental tests were done on the trimaran model to investigate the drag force in the range of low to moderate Fr number: 0.21 to 0.51. To this aim, the side hulls are located at the middle part of the main hull and the transversal positions were varied with two configurations, 125 mm (configuration 1) and 150 mm (configuration 2) away from the main hull (see table 3 and 4).

Table 2. Drag force measured for the trimaran with configuration 1 for the Fr 0.21~0.51.

	Configuration 1						
Fr_n	0.21	0.26	0.31	0.36	0.41	0.46	0.51
Drag(N)	99	NA	123	226	245	375	411

Table 3. Drag force measured for the trimaran with configuration 2 for the Fr 0.21~0.51.

	Configuration ٢						
Fr_n	0.21	0.26	0.31	0.36	0.41	0.46	0.51
Drag(N)	41	86	120	151	189	226	251

According to table 3 by increasing the Fr number the drag force increases. Moreover even a slight increase in the transversal position of the side hull (config. 1 to config. 2) causes a reduction on trimaran drag force. The reason might be based on the fact that by increasing the distance between side hull and man hull the wave interaction produced by each hull decreases; more over by approaching the hulls to each other (config. 1) the trapped wakes between the hulls will have less space to be damped and thus generate another source of drag increment. The numerical simulation was validated by comparing with the experimental results. To this aim a parameter: the ratio of the drag of various velocity to the drag of the lowest velocity related to Fr = 0.21 is introduced as criterion factor. For this reason two cases of trimaran configuration were studied:

case I, the side hulls are at 9.6 meter transversal distance and 18 meter longitudinal distance (corresponding to model trimaran with 200 mm longitudinal and 125 mm transversal side hull position) and case II, the side hulls are in 12 meter transversal distance and exactly at the rear position of the main hull (corresponding to model trimaran with 0 mm longitudinal and 150 mm transversal side hull position). The result of such comparison is provided below (Figures 7 and 8):

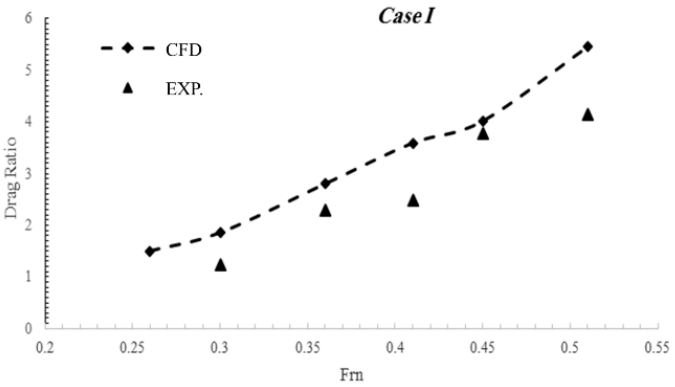


Figure. 7 The Drag ratio of case I for the data derived from the numerical approach and resulted from the experimental setup

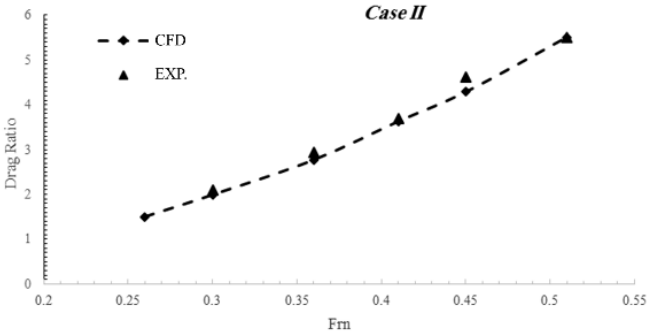


Figure. 8The Drag ratio of case II for the data derived from the numerical approach and resulted from the experimental setup

The drag ratio is defined as$\frac{C_d}{C_{d0}}$, while C_{d0} is the total drag at Fr= 0.21, the available experimental results are up to Fr number 0.51. There is a good agreement between the trends of the two diagrams. At case I , the numerical approach shows a bit of overestimation however both diagrams show peak and valley, though the numerical results is more flattened relatively and the valley value is seen in higher Fr number. The reason for the more scattered type data of the experimental result is due to the fact that it also concludes the wave phenomenon, conversely the numerical approach may poorly capture such event. As seen in case II when the side hull is positioned at the rear part of the main hull together with the higher transversal distance, the experimental result has an ascending trend with almost constant slope which is also repeated in the numerical approach result. Here however the numerical approach underestimates the Drag ratio. The almost constant slope at case II compared to a slightly slope fluctuation at case I reveals the effect of positioning the side hull at the middle part of the main hull, that is, the effect of wave making, wave breaking and wave interaction may play a role; in specific the longitude positioning of the side hull is the source of wave making or wave breaking and the transverse closeness is the source of the wave interaction. Thus due to further transverse distance of the side hull to the main hull as well as positioning at the rear part of the main hull at case II caused less fluctuation over the drag ratio. As of the aim of the current study, our investigation was focused

[Downloaded from ijmt.ir on 2026-11-25]

to optimize the longitudinal position of the side hull for two main cases, say, side hull transverse position: Y1= 9.6 m and Y2= 12m. The side hull accordingly advances step by step toward the front of the main hull and until it reaches to the middle of the main hull of the trimaran. More advancing the position of the side hull was not the purpose of this study. More precisely several trimaran were modeled while the side hulls are moved from the very rear part of the main hull to 40% of the length of the trimaran. The optimization parameter is the total drag consists of the pressure and viscous drag. Here the results based on the total drag are provided. It can be seen that how the trimaran behaves sometimes with radical drag variations with respect to the trimaran side hulls position and the Fr number. A wide range of Fr number from very low to very high value were examined through the numerical approach; Fr number equal to 0.15, 0.30, 0.45, 0.60, 0.75, 0.90 and 1.

Figures 9 depict the variations of total drag versus longitudinal position of the side hull for various Fr number when the transversal distance is Y1= 9.6 m

An overall look on the total drag diagram with variations of Fr number indicates that in general the total drag increases by increasing the Fr number however in some Fr numbers such as 0.15, 0.45, 0.6 and 1 the slope of the diagram turns down when the side hulls get close to the middle part of the main hull. By moving the side hull from the rear part to the front part of the trimaran, the total drag varies in three stages; at first and the last stage the total drag variation slope is low while between those stages the variation slope is very high. Thus moving the side hull from the rear part to somewhere around 25% of the length of the main hull causes the highest level of total drag in most of the cases. In particular at Fr number 0.15 and 0.6 at the first stage the drag either decrease or does not increase. At the last stage again there is a reduction in drag force. Fr number 0.3 and 0.75 show an always ascending diagram. At Fr number 0.45 the total drag diagram is ascending until close to the middle of the trimaran at which the total drag slightly decreases.

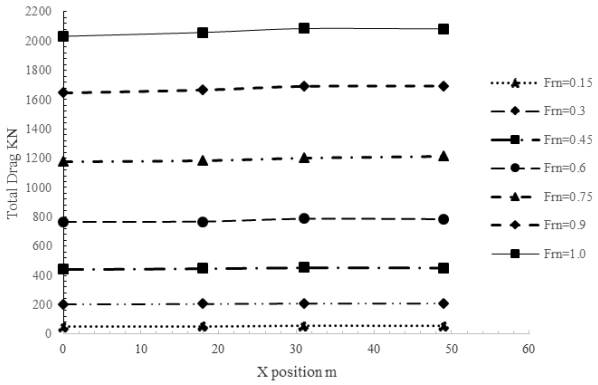


Figure. 9 The variation of total drag vs. x position of the side hull at Fr number when the transversal distance is Y1= 9.6 m

Figures 10 depict the variations of total drag versus longitudinal position of side hull for various Fr number when the transversal distance is Y2= 12m.

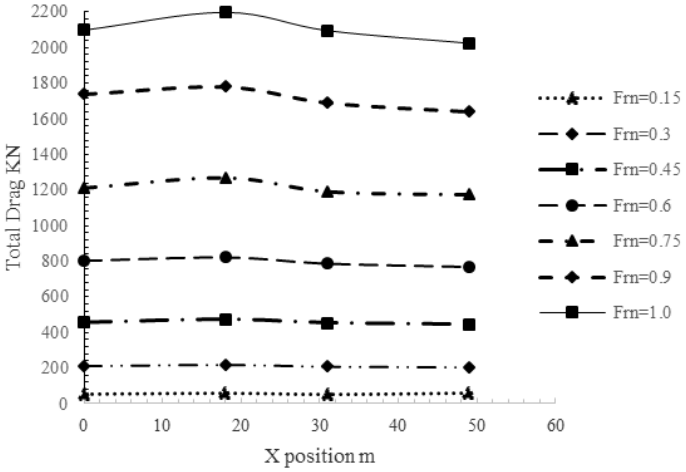


Figure. 10 The variation of total drag vs. x position of the side hull at Fr number when the transversal distance is Y1= 12 m

When the transversal distance is Y2=12 m, the case of Fr number 0.15 behaves in different way comparing to the rest of the Fr numbers, that is, at Fr number 0.15 there is an increase, decrease and again increase in total drag level versus advancing the side hull, though it should be considered that the total change in Fr number 0.15 is not so significant. For the rest of Fr numbers there is almost similar behavior: there is an increase of total drag followed by two stages of decrease in total drag with higher and lower slope respectively. By increasing the Fr number the variation of total drag versus side hull movement increases. Moreover the total drag value increases by increasing the Fr number.

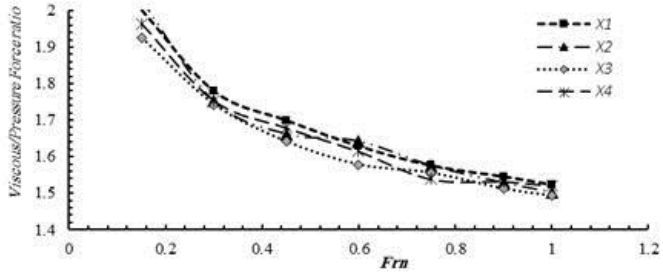


Figure. 11 Viscous to Pressure force ratio vs. Fr number for various side hull longitudinal position at Y1= 9.6 m.

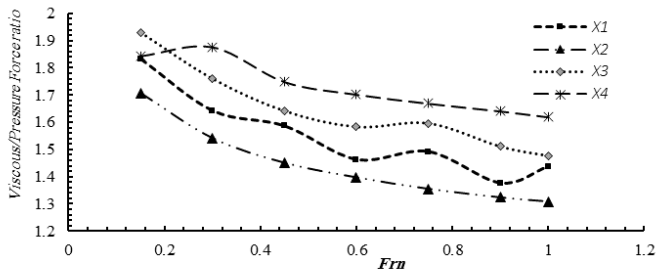
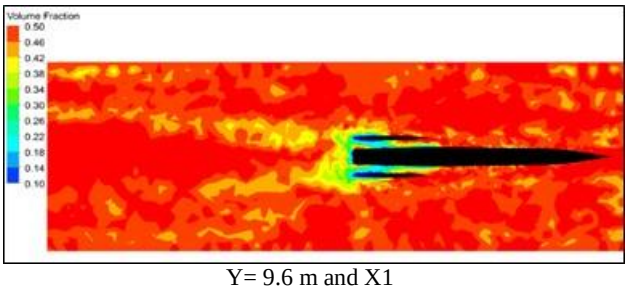


Figure. 12 Viscous to Pressure force ratio vs. Fr number for various side hull longitudinal position at Y2= 12m.

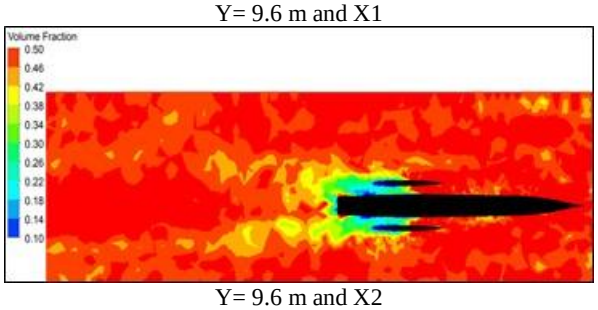
Figures 12 and 13 indicate the variation of Viscous to Pressure Force ratio versus Fr number based on the longitudinal and transversal position of the side hull

[Downloaded from ijmt.ir on 2026-11-25]

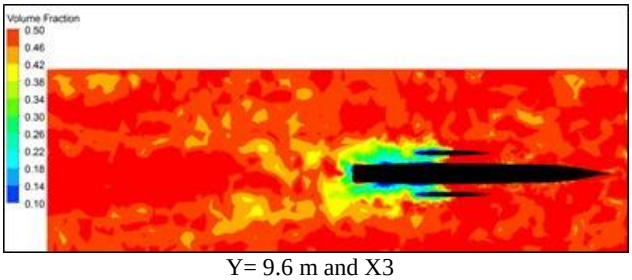
(longitudinal positions are here applied as X1=0 m, X2= 18 m, X3= 31 m and X4= 49 m away from the very rear part of the main hull). The viscous to pressure force ratio has a different behavior for the case of Y1 and Y2. At Y1 the variations of Viscous to Pressure Force ratio for various X do not differ very much. For both cases of Y1 and Y2 the diagram of the viscous to pressure force ratio is descending. The difference between the cases with different longitudinal values (X) at Y1 is much less than Y2. At Y2 although the trend of the diagram for the cases with different longitudinal values (X) are more or less similar the X1 has a different behavior in terms pf indicating more fluctuation. Moreover for X2 to X4 there is an increase on the level of viscous to pressure force ratio while this trend is not applicable considering for X1 to X2. Generally speaking the viscous to pressure force ratio is always bigger than 1 indicating that the viscous force in trimaran is bigger than the pressure force.



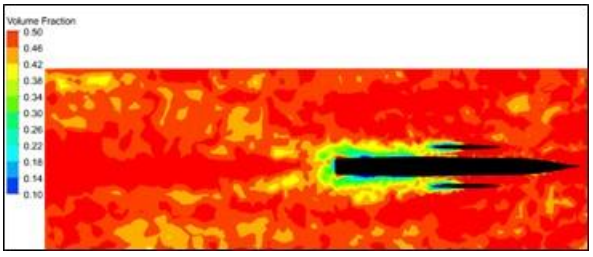
Y= 9.6 m and X1



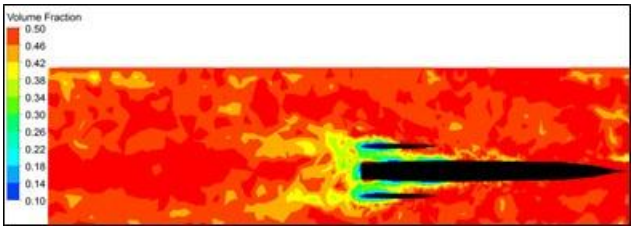
Y= 9.6 m and X2



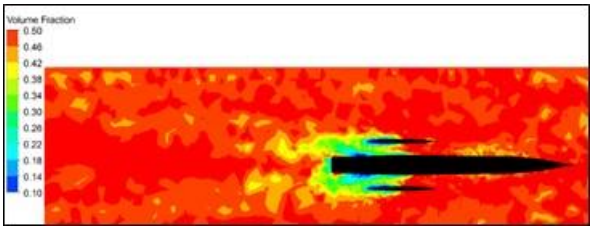
Y= 9.6 m and X3



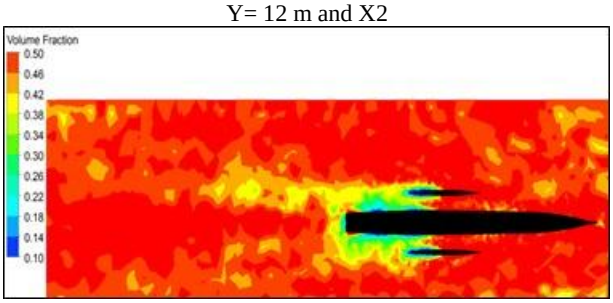
Y= 9.6 m and X4



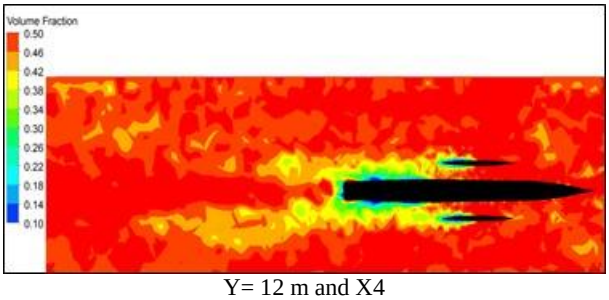
Y= 12 m and X1



Y= 12 m and X2



Y= 12 m and X3



Y= 12 m and X4

Figure. 13Volume of water fraction at plane of water/air initial level for trimaran different configurations

Figures 13 indicate thetypically volume of water fraction at the initial position of water/air levelin Fr0.45. These contours actually represent the peak and valley of the water as a consequence of wave production. A very slender shape of the main hull as well as the side hulls prevents any significant perturbation at the front side of the trimaran while conversely at the aft part of both the main hull and side hulls lots of perturbations are created. Thus for the configurations of which the side hull is located closer to the aft, the total area affected by such perturbation pattern is widened and limited to the aft part, conversely by moving the side hull toward the front part of the main hull the affected area is lengthened but also narrowed which attached to the main hull. Moreover by increasing the transversal distance of the side hull, the perturbation widened and also lengthened toward the aft of the trimaran and affected far domain beyond that of closer transversal side hull case (Y=9.6 m).

[Downloaded from ijmt.ir on 2026-11-25]

7. Conclusion

In this study an experimental setup as well as numerical approach (CFD) was exploited in order to predict the flow pattern and total drag level based on the various configuration of side hulls on a trimaran with a new hull profile: „wave piercing bow". The results of the CFD study had a good agreement with those of experimental setup. Via current study it was concluded that the various configuration shows different flow pattern and more importantly different total drag value. More specifically the trend and value of total drag changes based on the Fr number and so the trimaran velocity. This fact in particular suggests that any newly modification of the trimaran should be applied considering the desired velocity. Furthermore the total drag number increases rapidly by increasing the Fr number indicating more design effort for the trimaran modification at higher speed. The flow pattern and the produced wave is also depends on the side hull at which by approaching the side hull to the main hull the affected area narrowed and became smaller, conversely the higher transversal distance causes the affected area stretched to the aft of the trimaran although the wave interaction may reduce. Furthermore, moving the side hull toward the front part of the main hull causes the affected area stretched toward the front side however it narrowed and somewhat limited around and attached to the hull wall area.

8. References

1-Elcin, Z.; (2003), *Wave making resistance characteristics of trimaran hulls*: Ms Thesis; Naval Postgraduate School, Monterey, California, Available from Internet:
www.dtic.mil/dtic/tr/fulltext/u2/a420575.pdf

2- Maki, K.J. et al.; (2007),*Resistance Predictions for a High-Speed Sealift Trimaran,* 9th Int. Conf. on Numerical Ship Hydrodynamics Ann Arbor, Michigan, Aug. 5-8.
www.dtic.mil/dtic/tr/fulltext/u2/p023922.pdf

3- Hebblewhite, K.; Sahoo, P. K.; Doctors, L.J. (2007),*A case study: theoretical and experimental analysis of motion characteristics of a trimaran hull form*, SAOS Vol. 2 No. 2 pp. 149–156.
http://dx.doi.org/10.1080/17445300701430242

4- Fang, M.C.; Chen, T.Y. (2008),*A parametric study of wave loads on trimaran ships traveling in waves*, Ocean Engineering 35: 749–762.
http://dx.doi.org/10.1016/j.oceaneng.2008.02.001

5- Javanmardi, M.R.; Jahanbakhsh, E.; Seif, M.S.; Sayyaadi, H. (2008),*Hydrodynamic Analysis of Trimaran Vessels*, Polish Maritime Research 1(55) Vol 15; pp. 11-18. DOI: 10.2478/v10012-007-0046-5

6- Vakilabadi K. A.; Khedmati, M.R.; Seif, M.S. (2014),*Experimental Study on Heave and Pitch Motion Characteristics of A Wave-Piercing Trimaran*, Transactions of FAMENA 38 (3), 13-26. http://hrcak.srce.hr/129609

7- Mizine, I.; Karafiath, G.; Queutey, P.; Visonneau, M. (2009),*Interference Phenomenon in Design of Trimaran Ship*, 10th International Conference on Fast Sea Transportation, FAST, Athens, Greece.

8- Chong-ben, N.; Ren-chuan, Z.; Guo-ping, M.; Ju, F. (2011),*Hull Gesture and Resistance Prediction of High-Speed Vessels*, J. of Hydrodynamics, 23(2):234-240. DOI: 10.1016/S1001-6058(10)60108-4

9- Bo, Y.; Zuo-chao, W.; Ming, W. (2012),*Numerical Simulation of Naval Ship's Roll Damping Based on CFD*, The Second SREE Conference on Engineering Modelling and Simulation, Procedia Engineering 37: 14 – 18, Elsevier. doi:10.1016/j.proeng.2012.04.194

10- Zeraatgar, H.; Vakilabadi, K.A.; Yousefnejad, R. (2011),*Parametric Analysis of Ship Squat in Shallow Water by Model Test*, Brodogradnja 62 (1), 37-43.

[Downloaded from ijmt.ir on 2026-11-25]